

METAMORPHISM AND CO₂-PRODUCTION IN COLLISIONAL OROGENS: CASE STUDIES FROM THE HIMALAYAS

GIULIA RAPA

Dipartimento di Scienze della Terra, Università di Torino, Via Valperga Caluso 34, 10125 Torino

PROBLEM STATEMENT AND AIMS

Understanding the processes controlling the nature and magnitude of CO₂ global cycle is fundamental for the comprehension of the past-to-present global climate changes (Evans, 2011). The “long-term carbon cycle” (Berner, 1999) operates over millions of years and involves the slow exchange of carbon between rocks and the surficial systems (oceans, atmosphere, biota and soils); it is worth of attention for the huge volume of CO₂ possibly involved (Kerrick & Caldeira, 1993; Evans, 2011; Gaillardet & Galy, 2008; Skelton, 2013).

So far, the CO₂ degassing flux was mainly estimated based on the CO₂ emitted by volcanoes in different geodynamic contexts, magmatic CO₂ derived from the mantle and metamorphic CO₂ degassed from subduction zones. This estimated flux does not take into account CO₂ derived from orogenic zones, where it is formed through metamorphic reactions between carbonates and silicates. Primary geologic settings for the production of significant amounts of metamorphic CO₂ include collisional contexts where decarbonation reactions occur at relatively high temperatures within metacarbonate rocks (*e.g.*, calc-silicate rocks and impure marbles, derived from carbonate-rich pelites, marls, impure limestones and/or dolostones). The nature and magnitude of metamorphic CO₂ cycle, however, is still poorly understood and remains difficult to be defined (Gaillardet & Galy, 2008; Skelton, 2013; Groppo *et al.*, 2013, 2017; Rolfo *et al.*, 2015).

The Himalayan belt is the largest “large-hot” collisional orogen on Earth, where tectonic processes are still active. The medium to high geothermal gradients experienced (at least in the central and eastern sectors of the orogen; Goscombe *et al.*, 2006) during the Himalayan continental collision, may have allowed the release of metamorphic CO₂ through prograde devolatilization reactions. Moreover, CO₂-source rocks are widespread at different structural levels (Rolfo *et al.*, 2017): the Himalayan belt is therefore the ideal natural laboratory in which to study metamorphic CO₂-producing processes. However, the CO₂-producing lithologies in Himalaya have been largely ignored in previous petrological studies, being mainly mentioned as intercalations within the prevailing metapelitic sequences of the Lesser Himalayan Sequence and Greater Himalayan Sequence (*e.g.*, Goscombe *et al.*, 2006).

The aim of this PhD work was to achieve a deeper understanding of the role exerted by the Himalayan orogeny on the long-term global carbon cycle, clarifying the abundance, distribution and types of CO₂-source rocks in selected sectors of the Himalayan orogen, the nature of the metamorphic CO₂-producing reactions, the amounts of CO₂ produced through these reactions, and the chronology of the CO₂-producing reactions. To achieve these results, a detailed knowledge of the structural and metamorphic architecture of the selected sector of the Himalayan chain is mandatory.

TECTONO-STRATIGRAPHIC ARCHITECTURE AND METAMORPHIC EVOLUTION OF THE AREA

The study area is located in central Nepal, north of Kathmandu, in the Gatlang-Langtang and Gosainkund-Helambu regions. All the main tectono-metamorphic units of the Himalayan chain are exposed. From lower to upper structural level these are (Fig. 1): *i*) the Lesser Himalayan Sequence (LHS) and Ramgarh Thrust Sheet (LHS-RST), mainly consisting of phyllites and slates with intercalations of orthogneiss upsection; *ii*) the Lower Greater Himalayan Sequence (L-GHS), consisting of highly deformed garnetiferous schists and kyanite/sillimanite-bearing gneisses; *iii*) the Upper-Greater Himalayan Sequence (U-GHS) consisting of migmatites and granitic orthogneisses with bodies of leucogranites.

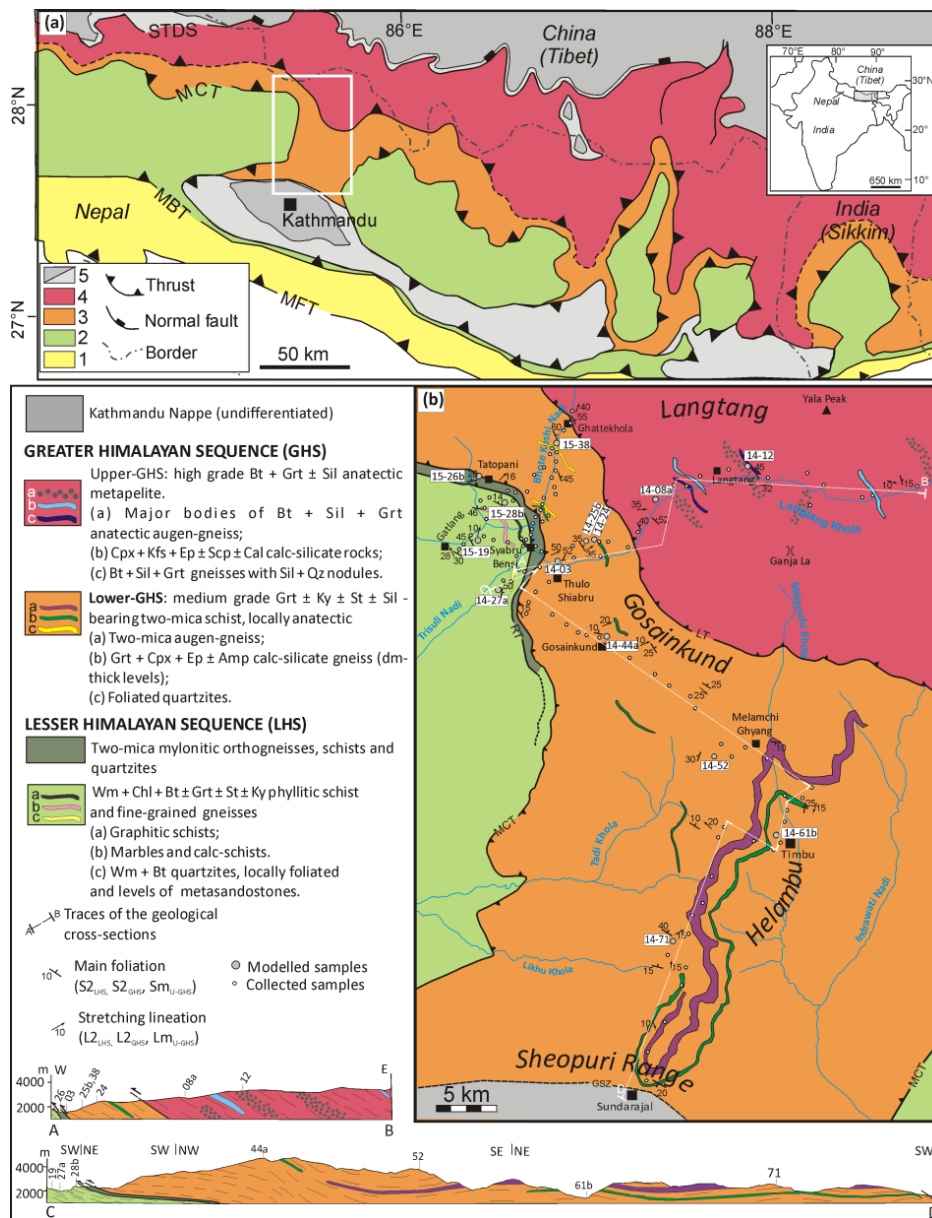


Fig. 1 - (a) Geological sketch map of the central-eastern Nepal Himalaya, with major tectono-metamorphic units (modified from Goscombe *et al.*, 2006, He *et al.*, 2015, Wang *et al.*, 2016 and based on our own data). The white rectangle indicates the study area, reported in (b). 1: Siwalik deposits; 2: Lesser Himalayan Sequence; 3: Lower Greater Himalayan Sequence; 4: Upper Greater Himalayan Sequence; 5: Tethyan Sedimentary Sequence. MFT: Main Frontal Thrust; MBT: Main Boundary Thrust; MCT: Main Central Thrust; STDS: South Tibetan Detachment System. The inset locates the study area in the framework of the Himalayan chain. (b) Geological map and representative cross sections of the Gatlang-Langtang and Gosainkund-Helambu regions (central Nepal Himalaya). GSZ: Galchi Shear Zone (from He *et al.*, 2015); RT: Ramgarh Thrust; MCT: Main Central Thrust; LT: Langtang Thrust.

In order to understand the structural and metamorphic architecture of both LHS and GHS in the study area, detailed fieldwork and petrological studies were performed along the Gosainkund-Helambu and Gatlang-Langtang transects.

Peak P-T conditions were estimated for selected metapelite samples using the pseudosection approach and the Average PT method on 14 samples (Fig. 2; Rapa *et al.*, 2016, 2018). The structurally lowest LHS samples have a metamorphic evolution characterized by a narrow hairpin P-T path with peak P-T conditions of

$595 \pm 25^\circ\text{C}$, 7.5 ± 0.8 kbar, corresponding to a T/depth ratio of $24 \pm 3^\circ\text{C}/\text{km}$ (using both the phase diagram approach and the Average PT approach). The structurally upper LHS samples belong to the LHS-RTS, which is characterized by a P-T evolution at higher P-T conditions ($635 \pm 15^\circ\text{C}$, 9.6 ± 1 kbar) and defines a lower T/depth ratio of $20 \pm 2^\circ\text{C}/\text{km}$ ($21 \pm 3^\circ\text{C}/\text{km}$ using Average PT).

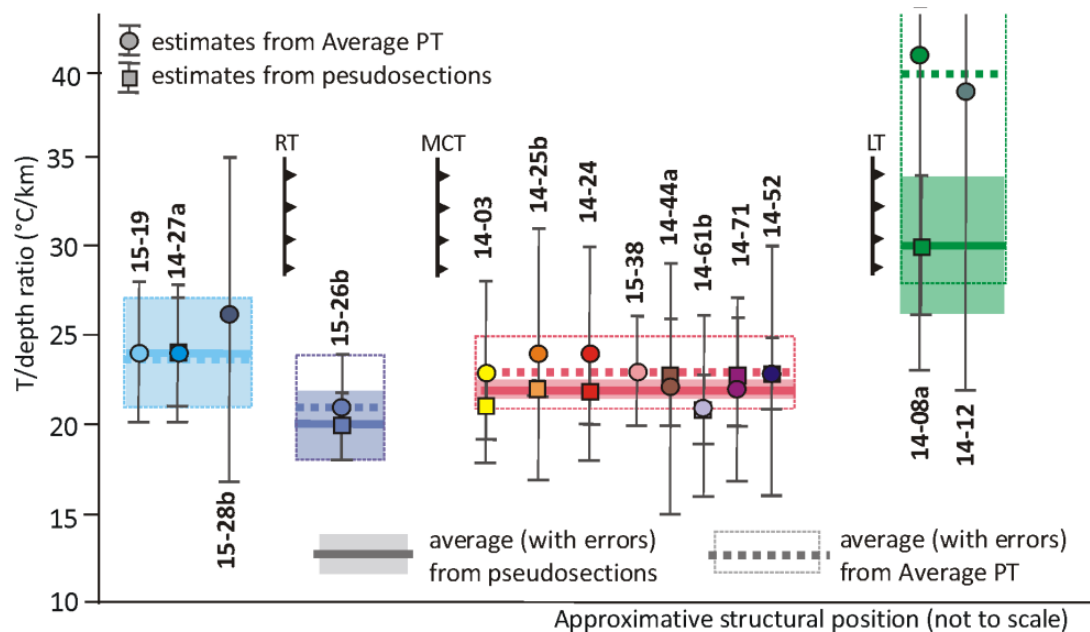


Fig. 2 - T/depth ratios ($^\circ\text{C}/\text{km}$) (with errors) plotted as a function of the (approximate) structural position for the samples. The lines (and coloured boxes) refer to the weighted mean values (and errors) obtained with the pseudosection approach; the dashed lines (and dashed boxes) refer to the weighted mean values (and errors) obtained with the Average PT method. RT: Ramgarh Thrust, MCT: Main Central Thrust, LT: Langtang Thrust.

Based on the difference in peak metamorphic conditions and T/depth ratios, the occurrence of a tectono-metamorphic discontinuity separating these two sets of samples is confirmed (*i.e.*, the Ramgarh Thrust, Fig. 2). Along the Gatlang-Langtang section, two tectono-metamorphic units have been distinguished within the GHS: L-GHS, characterized by peak P-T conditions at $725 \pm 4^\circ\text{C}$, 10 ± 0.1 kbar (corresponding to a T/depth ratio of $22 \pm 0.5^\circ\text{C}/\text{km}$; $23 \pm 2^\circ\text{C}/\text{km}$ using the Average PT approach), and the structurally higher U-GHS, with peak metamorphic conditions at $780 \pm 20^\circ\text{C}$, 7.8 ± 0.8 kbar (corresponding to a T/depth ratio of $30 \pm 4^\circ\text{C}/\text{km}$; $40 \pm 12^\circ\text{C}/\text{km}$ using the Average PT method). These data show the existence of a main tectono-metamorphic discontinuity within the GHS, as previously suggested by other authors. The LHS and GHS are in turn separated by the Main Central Thrust.

The Gosainkund-Helambu region occupies a key area for the development of Himalayan kinematic models, connecting the well-investigated Gatlang-Langtang area to the North with the Kathmandu Nappe, whose interpretation is still debated, to the South. The results of petrological modelling of the metapelites from the Gosainkund-Helambu section show that this region is entirely comprised within the L-GHS unit (Rapa *et al.*, 2016): the estimated peak metamorphic conditions of $737 \pm 8^\circ\text{C}$, 10 ± 0.4 kbar correspond to a uniform T/depth ratio of $23 \pm 1^\circ\text{C}/\text{km}$ ($22 \pm 3^\circ\text{C}/\text{km}$ using the Average PT approach). The metamorphic discontinuity identified along the Langtang transect and dividing the GHS in two tectono-metamorphic units is located at a structural level too high to be intersected along the Gosainkund-Helambu section. These results have significant implications for the tectonic interpretation of the Kathmandu Nappe (KN) and provide a contribution to the more general discussion of the Himalayan kinematic models. The structurally lower unit of the KN (known as Sheopuri Gneiss) can be correlated to the L-GHS unit; this result strongly supports those models that correlate

the KN to the Tethyan Sedimentary Sequence and that suggest the merging of the South Tibetan Detachment System and the Main Central Thrust on the northern side of the KN. In this sector of the Himalayan chain, the most appropriate kinematic model able to explain the observed tectono-metamorphic architecture of the GHS is the duplexing model, or hybrid models which combine the duplexing model with another end-member model.

METAMORPHIC CO₂-SOURCE ROCKS IN COLLISIONAL OROGENS: OCCURRENCE, TYPES AND PROTHOLITHS

Fieldwork performed in the study area and in eastern Nepal highlighted that CO₂-source rocks are widespread at different structural levels and occur as: decimeter- to meter- thick layers or boudins in both the LHS and the L-GHS, vs. tens to hundreds of meter thick layers within anatectic gneisses in the structurally upper U-GHS. Three different chemical groups were recognized, and they can be described in terms of relatively complex chemical systems: (1) CFMAST-HC (CaO-FeO-MgO-Al₂O₃-SiO₂-TiO₂-H₂O-CO₂) group, significantly more abundant in the U-GHS; (2) NCFMAST-HC (Na₂O-CaO-FeO-MgO-Al₂O₃-SiO₂-TiO₂-H₂O-CO₂) and (3) NKCFMAST-HC (Na₂O-K₂O-CaO-FeO-MgO-Al₂O₃-SiO₂- TiO₂-H₂O-CO₂) groups, widespread in both the GHS (L-GHS and U-GHS) and LHS. In all groups, mineral assemblages vary with increasing metamorphic grade from lower to upper structural levels. Different petrographic types were distinguished for each chemical group, based on the mineral assemblages (*i.e.*, Types 1A to D; Types 2A-2B; Types 3A to F). Most of these assemblages, especially those equilibrated at lower temperatures and still containing abundant phyllosilicates, are not easy to recognize in the field and were probably considerably overlooked by previous studies.

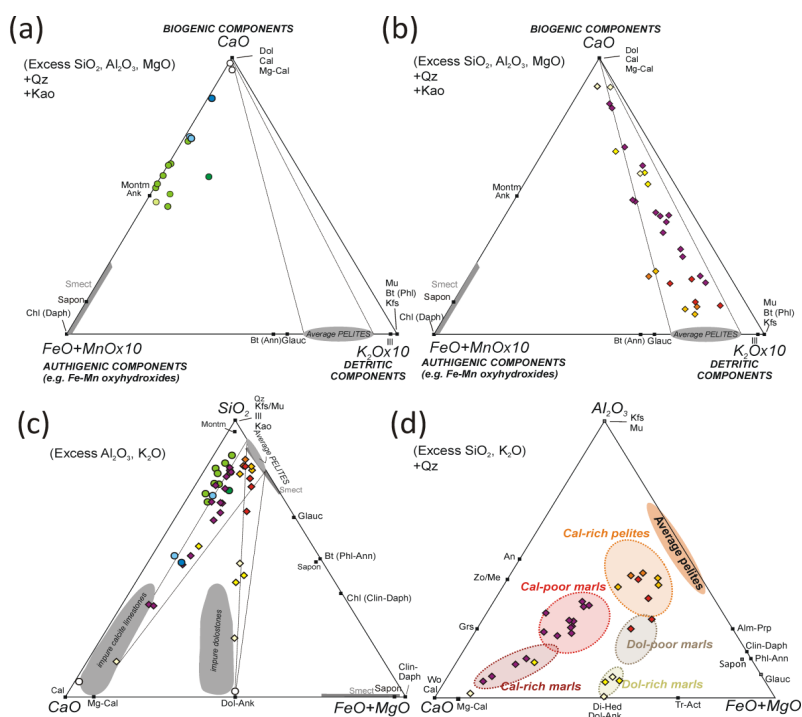


Fig. 3 - Diagrams of bulk-rock compositions for the analysed CO₂-source rock samples. (a,b) CaO-K₂O x10-(FeO+MnO x10) diagrams for the (N)CFMAST-HC (a) and NKCFMAST-HC (b) groups, highlighting the different mineralogical components of the protoliths. The “Average pelite composition” field derives from bulk rock compositions of metapelites from this study (see also Rapa *et al.*, 2016). (c) CaO-SiO₂-(FeO+MgO) diagram for both the (N)CFMAST-HC and NKCFMAST-HC groups. Compositional fields of impure calcitic limestones and dolomites are from Tracy & Frost (1991). (d) Al₂O₃-CaO-(FeO+MgO) diagram for Type 3 of CO₂-source rocks, highlighting Mg-calcite and dolomite -derived sediments.

Major and trace element patterns suggest that CO₂-source rocks belonging to the NKCFMAST-HC group derive from a marly protolith, with variable modal amounts of biogenic (carbonatic) and pelitic components (Fig. 3b-d). On the contrary, CO₂-source rocks belonging to the CFMAST-HC and NCFMAST-HC groups show a significantly different trend (Fig. 3a), suggesting that their protoliths were smectite-rich bentonites, possibly deriving from the alteration of volcanic ash layers.

PETROLOGICAL MODELLING OF CO₂-SOURCE ROCKS AND TIMING OF CO₂-FLUXES

The phase petrology approach was used to investigate the most relevant CO₂-producing reactions in different types of CO₂-source rocks (Type 1C, 3C, and 3F) and to quantify the amounts of CO₂ that were released through these reactions. This approach allowed an indirect estimate of the amount of CO₂ released during prograde metamorphism. The thermodynamic modelling of metacarbonate rocks is challenging: the main difficulties are related to the presence of a H₂O-CO₂ fluid, whose composition is an additional variable, and to the common occurrence of complex Mg-Fe-Ca (garnet, clinopyroxene, amphibole) and Ca-Na (plagioclase, scapolite) solid solutions, as well as of K-bearing phases (white mica, biotite, K-feldspar) and Ti-bearing phases (biotite, titanite). Decarbonation reactions were modelled in the CFMAST-HC system and in the more complex MnNKCFMAST-HC and NKCFMAST-HC systems using different types of phase diagrams: P/T-XCO₂ pseudosections, P/T-XCO₂ sections and mixed-volatile P-T phase diagrams. P-T data (*i.e.*, P/T gradient) obtained from the metapelites hosting the CO₂-source rocks were used.

In Type 1C sample (likely deriving from bentonite), the CO₂-producing process was a continuous process, and mostly occurred at relatively high T conditions. The final CO₂ production was lower than 1 wt.% of CO₂ (Fig. 4a, b), and more likely almost negligible because at least some of the CO₂-rich fluid internally produced during the prograde evolution of this sample remained confined within the system, allowing carbonation reactions to proceed at decreasing P-T conditions.

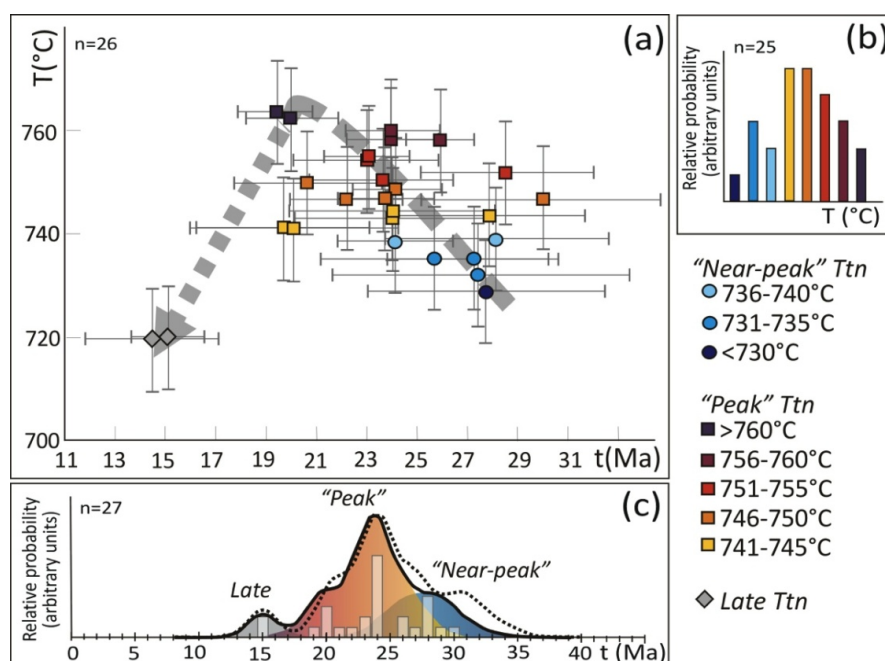


Fig. 4 - (a) P/T-X(CO₂) pseudosection for sample 14-44c (Type 1C), with the P-T-X(CO₂) evolution inferred and the modelled CO₂ (wt.%) amounts. (b) Modelled CO₂ amount (wt.%) and fluid composition along the P-T-X(CO₂) path of (a) with the maximum CO₂ production. (c) P/T-X(CO₂) pseudosection for sample 15-46 (Type 3C), with the P-T-X(CO₂) evolution inferred and the modelled CO₂ (wt.%) amounts. (d) Modelled CO₂ amounts (wt.%) and fluid composition along the three P-T-X(CO₂) paths. (e, g) P/T-X(CO₂) pseudosection for sample 14-53c and 14-17 (Type 3F), with the P-T-X(CO₂) evolution inferred and the modelled CO₂ (wt.%) amounts. (f, h) Modelled CO₂ amounts (wt.%) and fluid composition along the three P-T-X(CO₂) paths.

In Type 3C sample (derived from calcite-rich pelite) the majority of CO₂ (~2.5 wt.%) was released through continuous reactions occurring at relatively low P-T conditions (T < 500°C; P < 6 kbar), during the early prograde evolution (Fig. 4c,d). A small amount of CO₂ (< 0.5 wt.%) was additionally produced at ~500°C through a garnet-forming, calcite-consuming, discontinuity reaction. Overall, the CO₂ productivity of this sample is therefore < 3.5 wt.%.

In Type 3F lithologies (derived from marly protoliths) CO₂ was produced through distinct, short-lived events, which occurred at specific P-T conditions along the whole prograde metamorphic evolution, and especially at relatively high temperature (Fig. 4e-h). The predicted amounts of produced CO₂ are quite high (from a minimum of 2 wt.% to > 8 wt.% of CO₂) and vary as a function of the bulk composition.

Most of the CO₂-producing reactions modelled in the Type 3F CO₂-source rocks also produced titanite. Taking advantage of the possibility of simultaneously applying U-Pb geochronology and Zr-in-titanite thermometry, sample 14-53c was selected as a case study for constraining the timing of CO₂ production in the most abundant type of CO₂-source rocks within the GHS (Rapa *et al.*, 2017). Titanite grains grew during two nearly consecutive episodes of titanite formation: a near-peak event at 730-740°C, 10 kbar, 30-26 Ma, and a peak event at 740-765°C, 10.5 kbar, 25-20 Ma (Fig. 5).

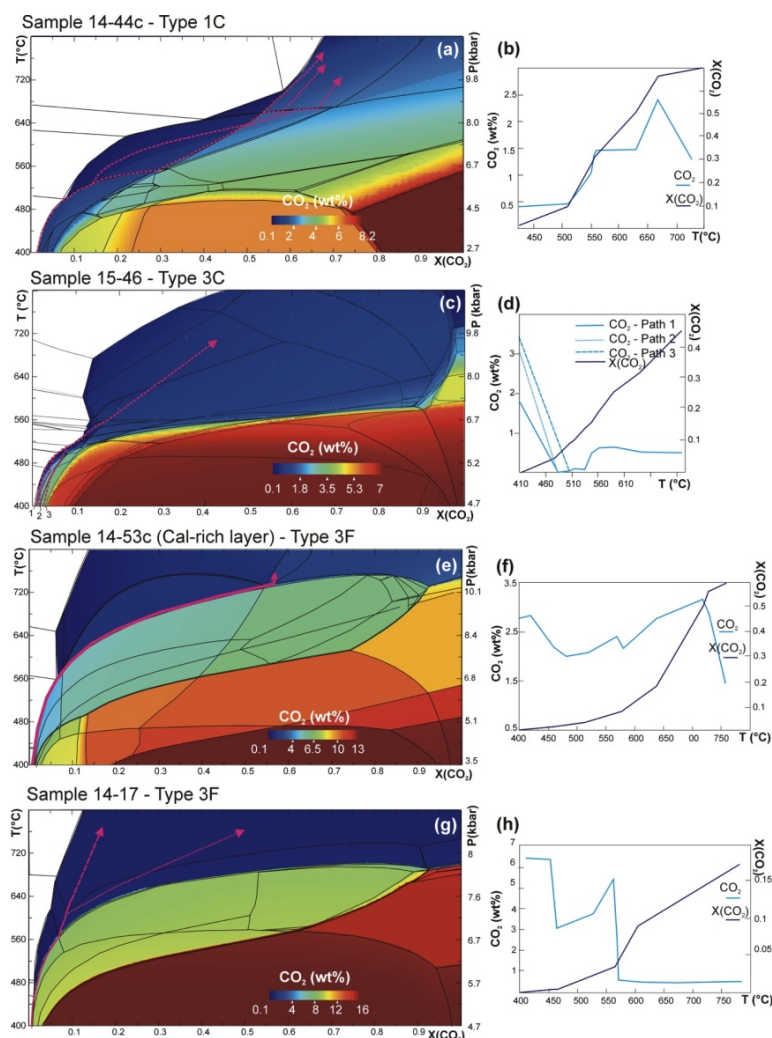


Fig. 5 - (a) Temperature-time diagram for sample 14-53c, showing gradually increasing temperatures between 28 and 19 Ma and a retrograde cooling at 15 Ma (grey symbols refer to the retrograde titanite generation). Errors on temperatures are $\pm 10^\circ\text{C}$. (b) Frequency distribution of Zr-in-titanite temperatures; the two titanite grains interpreted as retrograde are not considered, due to the uncertainties in the estimate of their temperature of crystallization. (c) Probability density plot for U-Pb ages (common $^{207}\text{Pb}/^{206}\text{Pb} = 0.84$); although partially overlapped, the “near peak” and “peak” titanite generations are clearly distinguishable. The dotted line refers to titanite ages obtained for a higher common Pb value ($^{207}\text{Pb}/^{206}\text{Pb} = 0.9$).

ESTIMATING CO₂-FLUXES FROM THE HIMALAYAS

In order to extrapolate the amount of produced CO₂ to the orogen scale (Table 1), an estimate of the total volume of this type of CO₂-source rocks in the whole Himalayan belt is needed, as well as the total volume of the GHS itself. Type 3F are by far the easiest to be recognized in the field, therefore they have been used as a starting point for the calculation. Considering the uncertainties associated with all the input values (volume of the whole GHS unit; vol% of the CO₂-source rocks; CO₂ productivity; duration of CO₂-producing process), the metamorphic CO₂ flux resulting from the studied CO₂-source rocks ranges between a minimum value of 1.4 Mt/yr and a maximum value of 19.4 Mt/yr. This estimated metamorphic CO₂ flux is of the same order of magnitude as present-day degassing from hot springs (Evans *et al.*, 2008: 8.8 Mt/yr), thus suggesting that CO₂-producing processes similar to those described in this Project still occur along the active Himalayan orogen (*e.g.* Girault *et al.*, 2014a, b).

Table 1 - Sensitivity analysis for the metamorphic CO₂ flux from the GHS Sequence of Himalaya

Variables	Values used in this paper	Max duration of CO ₂ -producing process	Max V GHS	Max Vol% calc-silicate rocks	Max CO ₂ productivity	Max CO ₂ flux
V GHS (km ³)	5.0E+06 ^a	5.0E+06	9.0E+06 ^c	5.0E+06	5.0E+06	9.0E+06
Vol% calc-silicate rocks (%)	10	10	10	20	10	20
CO ₂ productivity (Wt% CO ₂)	3	3	3	3	4	4
Duration of the CO ₂ -producing process (Ma)	20 ^b	30	20	20	20	20
CO₂ flux* (Mt/yr)	2.0	1.4	3.6	4.1	2.7	9.7
Total CO₂ flux[§] (Mt/yr)	< 4	< 3	< 7	< 8	< 5	< 19

* CO₂ flux from the studied calc-silicate rock type (*i.e.* derived from marly protoliths); [§] Total CO₂ flux, including the contribution of other CO₂ source rocks (*i.e.* derived from Cal-rich pelitic protoliths). Grey cells correspond to the variable parameters. a): Long *et al.*, 2011; b): Kohn, 2014; c): Kerrick & Caldeira, 1999.

To my knowledge, this is the first time that CO₂-producing metamorphic processes occurring during an orogenic event have been fully characterized in term of P-T conditions, time, duration and amounts of CO₂ produced. Although the volumes of the CO₂-source rocks involved in such processes could be potentially better constrained in the future, it is suggested that these metamorphic CO₂ fluxes should be considered in any future attempts of estimating the global budget of non-volcanic carbon fluxes from the lithosphere

REFERENCES

- Berner, R.A. (1999): A new look at the long-term carbon cycle. *GSA Today*, **9**, 1-6.
- Evans, K.A. (2011): Metamorphic carbon fluxes: how much and how fast? *Geology*, **39**, 95-96.
- Evans, M.J., Derry, L.A., France-Lanord, C. (2008): Degassing of metamorphic carbon dioxide from the Nepal Himalaya. *Geochem., Geophys., Geosys.*, **9**, Q04021.
- Gaillardet, J. & Galy, A. (2008): Himalaya-carbon sink or source? *Science*, **320**, 1727-1728.
- Girault, F., Bollinger, L., Bhattarai, M., Koirala, B.P., France-Lanord, C., Rajaure, S., Gaillardet, J., Fort, M., Sapkota, S.N., Perrier, F. (2014a): Large-scale organization of carbon dioxide discharge in the Nepal Himalayas. *Geophys. Res. Lett.*, **41**, 6358-6366.
- Girault, F., Perrier, F., Crockett, R., Bhattarai, M., Koirala, B.P., France-Lanord, C., Agrinier, P., Ader, M., Fluteau, F., Gréau, C., Moreira, M. (2014b): The Syabru-Bensi hydrothermal system in central Nepal: 1. Characterization of carbon dioxide and radon fluxes. *J. Geophys. Res.-Sol. Ea.*, **119**, doi:10.1002/2013JB010301.
- Goscombe, B., Gray, D., Hand, M. (2006): Crustal architecture of the Himalayan metamorphic front in eastern Nepal. *Gondwana Res.*, **10**, 232-255.
- Groppo, C., Rolfó, F., Castelli, D., Connolly, J.A.D. (2013): Metamorphic CO₂ production from calc-silicate rocks via garnet-forming reactions in the CFAS-H₂O-CO₂ system. *Contrib. Mineral. Petr.*, **166**, 1655-1675.
- Groppo, C., Rolfó, F., Castelli, D., Mosca, P. (2017): Metamorphic CO₂ production in collisional orogens: petrologic constraints from phase diagram modeling of Himalayan, scapolite-bearing, calc-silicate rocks in the NKC(F)MAS(T)-HC system. *J. Petrol.*, **58**, 53-83.

- He, D., Webb, A.A.G., Larson, K.P., Martin, A.J., Schmitt, A.K. (2015): Extrusion vs. duplexing models of Himalayan mountain building. 3: duplexing dominates from the Oligocene to Present. *Int. Geol. Rev.*, **57**, 1-27.
- Kerrick, D.M. & Caldeira, K. (1993): Paleoatmospheric consequences of CO₂ released during early Cenozoic regional metamorphism in the Tethyan orogen. *Chem. Geol.*, **108**, 201-230.
- Kerrick, D.M. & Caldeira, K. (1999): Was the Himalayan orogen a climatically significant coupled source and sink for atmospheric CO₂ during the Cenozoic? *Earth Planet. Sc. Lett.*, **173**, 195-203.
- Kohn, M.J. (2014): Himalayan metamorphism and its tectonic implications. *Ann. Rev. Earth Pl. Sc. Lett.*, **42**, 381-419.
- Long, S.L., McQuarrie, N., Tobgay, T., Grujic, D. (2011): Geometry and crustal shortening of the Himalayan fold-thrust belt, eastern and central Bhutan. *GSA Bull.*, **123**, 1427-1447.
- Rapa, G., Groppo, C., Mosca, P., Rolfo, F. (2016): Petrological constraints on the tectonic setting of the Kathmandu Nappe in the Langtang-Gosainkund-Helambu regions, central Nepal Himalaya. *J. Metamorph. Geol.*, **34**, 999-1023.
- Rapa, G., Groppo, C., Rolfo, F., Petrelli, M., Mosca, P., Perugini, D. (2017): Titanite-bearing calc-silicate rocks constrain timing, duration and magnitude of metamorphic CO₂ degassing in the Himalayan belt. *Lithos*, **292-293**, 364-378.
- Rapa, G., Mosca, P., Groppo, C., Rolfo, F. (2018): Tectono-metamorphic discontinuities within the Himalayan orogen: structural and petrological constraints from Rasuwa District, Central Nepal Himalaya. *J. Asian Earth Sci.*, **158**, 266-286.
- Rolfo, F., Groppo, C., Mosca, P., Ferrando, S., Costa, E., Kaphle, K.P. (2015): Metamorphic CO₂ degassing in the active Himalayan orogen: exploring the influence of orogenic activity on the long-term global climate changes. In: "Engineering Geology for Society and Territory - Volume 1 - Climate Change and Engineering Geology", G. Lollino, A. Manconi, J. Clague, W. Shan, M. Chiarle, eds. Springer International Publishing, Switzerland, 21-25.
- Rolfo, F., Groppo, C., Mosca, P. (2017): Metamorphic CO₂ production in calc-silicate rocks from the eastern Himalaya. *Ital. J. Geosci.*, **136**, 28-38.
- Skelton, A. (2013): Is orogenesis a net sink or source of atmospheric CO₂? *Geol. Today*, **29**, 102-107.
- Tracy, R.J. & Frost, B.R. (1991): Phase-Equilibria and Thermobarometry of Calcareous, Ultramafic and Mafic Rocks, and Iron Formations. *Rev. Mineral.*, **26**, 207-289.
- Wang, J.-M., Zhang, J.-J., Liu, K., Wang, X.-X., Rai, S., Scheltens, M. (2016): Spatial and temporal evolution of tectonometamorphic discontinuities in the Central Himalaya: constraints from P-T paths and geochronology. *Tectonophysics*, **679**, 41-60.